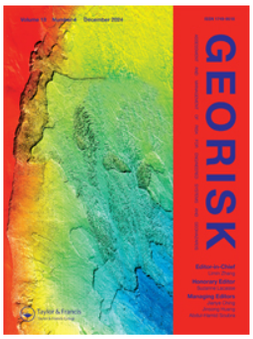

Taylor & Francis
Taylor & Francis Group

Georisk: Assessment and Management of Risk for Engineered Systems and Geohazards

ISSN: (Print) (Online) Journal homepage: www.tandfonline.com/journals/ngrk20

Characterisation of the spatial variability of underconsolidated Singapore Marine Clay using random field theory

Ze Zhou Wang, Xiangfeng Guo & Yue Hu

To cite this article: Ze Zhou Wang, Xiangfeng Guo & Yue Hu (11 Nov 2024): Characterisation of the spatial variability of underconsolidated Singapore Marine Clay using random field theory, Georisk: Assessment and Management of Risk for Engineered Systems and Geohazards, DOI: 10.1080/17499518.2024.2422487

To link to this article: https://doi.org/10.1080/17499518.2024.2422487

Published online: 11 Nov 2024.

GEORISK
https://doi.org/10.1080/17499518.2024.2422487

Taylor & Francis
Taylor & Francis Group

NOTE

Characterisation of the spatial variability of underconsolidated Singapore Marine Clay using random field theory

Ze Zhou Wang [a], Xiangfeng Guo [b] and Yue Hu [c]

[a]Marie Skłodowska-Curie Fellow, Civil Engineering Division, Department of Engineering, University of Cambridge, Cambridge, UK; [b]School of Marine Science and Engineering, South China University of Technology, Guangzhou, People's Republic of China; [c]Institute for Risk and Reliability, Leibniz Universität Hannover, Hannover, Germany

ABSTRACT

This paper characterised the spatial variability of Singapore Kallang Formation Marine Clays using piezocone penetration test (CPT) data from the Marina South area. Both vertical and horizontal scales of fluctuation in undrained shear strength for two distinct clay units, Upper Marine Clay (UMC) and Lower Marine Clay (LMC), are calibrated for autocorrelation and semi-variogram functions. The Marina South area was reclaimed from the sea using fills placed in three phases from 1970s to 1990s and remains underconsolidated up to date. This study identified variations in the degree of consolidation across the area, which has led to variations in the undrained shear strength in this area. However, the variations in the degree of consolidation were found to have no noticeable influence on the vertical and horizontal scales of fluctuation of either UMC or LMC unit. The vertical scales of fluctuation of UMC and LMC units are 0.57 $\pm$ 0.3 m and 0.48 $\pm$ 0.17 m, respectively, while the horizontal scales of fluctuations are 148 $\pm$ 26 m and 138 $\pm$ 28 m, respectively. The present study contributes to the database of the statistical and spatial variability of marine clays and can provide useful guidance for assessing reliability of excavations and foundations in Marina South as well as other areas with similar geological settings.

ARTICLE HISTORY
Received 1 February 2024
Accepted 19 October 2024

KEYWORDS
Marine clay; spatial variability; scale of fluctuation; cone penetration test; stochastic models; statistic analysis

1. Introduction

As highlighted in Phoon and Kulhawy (1999), the three primary sources of uncertainties in geotechnical analysis include inherent variability, measurement error, and transformation uncertainty. The inherent variability is usually regarded as a type of aleatory uncertainty, resulting primarily from the random natural geologic processes that continually modify the soil mass in situ. The importance of accurately characterising this variability and understanding its impact on geosystems have been demonstrated in numerous existing studies (Guo et al. 2023, Jaksa 1995; Phoon and Kulhawy 1999; Pieczyńska-Kozłowska, Chwała, and Puła 2022; Stuedlein et al. 2012; Wang et al. 2019; Xu et al. 2023). In addition, measurement error and transformation uncertainty are also critical uncertainty sources that can influence geotechnical design and analysis. Measurement error could contain both aleatory and epistemic components. Epistemic measurement errors may arise due to equipment calibration issues or human errors, among others, which can be minimised through more accurate equipment and better measurement procedures. The aleatory component is typically caused by random testing effects and variations in instrument precision. Furthermore, the transformation uncertainty is incurred when field or laboratory measurements are transformed into design soil properties using empirical or other correlation models. For example, Ching and Phoon (2012) characterised generic transformation uncertainties and compared the analyses of a global database with results mentioned in previous studies. They further recommended a sufficiently large database to achieve stable estimates of the transformation uncertainties. Furthermore, Wang et al. (2017) employed a Bayesian method to calibrate a transformation model and explicitly considered measurement errors and multiple other epistemic uncertainties. Overall, these three uncertainty sources can significantly influence the design and analysis of geotechnical problems and should be duly accounted for in geotechnical engineering. This paper focuses on quantifying the inherent spatial variability in soil properties.

In existing literature, a large part of studies on spatial variability has been founded on random field theory (Li

CONTACT Yue Hu yue.hu@irz.uni-hannover.de Institute for Risk and Reliability, Leibniz Universität Hannover, Hannover 30167, Germany

et al. 2024; Phoon et al. 2022; Vanmarcke 1977; Zhao et al. 2023). Random Field Finite Element Method (RFFEM) has, therefore, become an increasingly popular tool due to its capability for simulating the effects of spatial variability of soils (Fenton and Griffiths 2002; Griffiths, Huang, and Fenton 2009; Sujawat and Kumar 2023). The generation of random fields typically relies on an autocorrelation function that quantifies the spatial correlation between two spatial points separated by a specific distance. A typical two-dimensional (2D) Gaussian random field can then be simulated based on the following parameters: (i) mean, μ; (ii) standard deviation, σ; (iii) vertical scale of fluctuation, δ_v; and (iv) horizontal scale of fluctuation, δ_h, for each soil property of interest.

Here the term "scale of fluctuation" is used to describe the spatial variability of a geomaterial. Correlation length, correlation distance, autocorrelation length and autocorrelation distance are other terms used by the geotechnical literature to refer to a similar meaning. All these terms, including scale of fluctuation, have been generally defined as the distance within which soil property values show relatively strong correlation (Phoon and Kulhawy 1999). However, the mathematical definitions of all these terms are not the same. Correlation length was first defined by Diaz Padilla and Vanmarcke (1974) as the distance at which the autocorrelation coefficient, for a single exponential function, decays to $[1/e]$. Correlation distance, autocorrelation length and autocorrelation distance have since been defined in a similar manner (Baecher et al. 1980; DeGroot and Baecher 1993; Qi and Liu 2019). In contrast, scale of fluctuation, introduced by Vanmarcke (1977), was defined mathematically as twice the area under the positive part of the autocorrelation function (Fenton 1999; Huber 2013; Jaksa 1995; Vanmarcke 1977). As a result, taking a single exponential autocorrelation function as an example, the scale of fluctuation is twice the magnitude of the correlation distance. This issue can be particularly important in practical implementation. For example, Optum G2 (Krabbenhoft, Lyamin, and Krabbenhoft 2015), a conventional FE program, requires the user to input correlation length for a single exponential autocorrelation function. A literature survey revealed that both terms have been commonly reported. Papers by Jaksa (1995); Jaksa, Brooker, and Kaggwa (1997); Jaksa, Kaggwa, and Brooker (1999); Phoon and Kulhawy (1999); Uzielli, Vannucchi, and Phoon (2005); Liu and Chen (2010); Dasaka and Zhang (2012); Firouzianbandpey et al. (2014); Oguz, Huvaj, and Griffiths (2019) all referred to scale of fluctuation while Baecher et al. (1980); Honjo (1982); DeGroot and Baecher (1993); Navin (2005); Qi and Liu (2019) referred to correlation length. In this study, conventional scale of fluctuation recommended by Vanmarcke (1977) is adopted as the parameter to describe spatial variability.

Table 1. Typical autocorrelation functions.

Model Name	Autocorrelation Function	**Scale of Fluctuation δ**
Single Exponential (SNX)	$\rho_{\Delta z} = e^{-\frac{\lvert\Delta z\rvert}{b}}$	$2b$
Squared Exponential (SQX)	$\rho_{\Delta z} = e^{-(\frac{\lvert\Delta z\rvert}{b})^2}$	$\sqrt{\pi}b$
Second-order Markov (SOM)	$\rho_{\Delta z} = e^{-(\frac{\lvert\Delta z\rvert}{b})}(1+\frac{\lvert\Delta z\rvert}{b})$	$4b$

Furthermore, Phoon and Kulhawy (1999) compiled a database of random field model parameters from an extensive literature review. However, the compiled parametric data corresponds to a limited set of geological environments and the obtained parametric intervals might be difficult to generalize in other geological settings. Further statistics have also been reported by Nishimura et al. (2017), Bong and Stuedlein (2018), and De Gast, Vardon, and Hicks (2021). A series of studies has also been carried out to determine the specific soil random field parameters for local-scale geological conditions. Various types of soil investigation data (standard penetration test SPT, field vane shear test VST and piezocone penetration test CPT) have been used to characterise spatial variability. Among different types of in situ test data, CPT data has been preferred over other types of soil investigation data (e.g. SPT, VST) for determining the random field parameters of soils mainly because it provides the finest vertical resolution. For example, DeGroot and Baecher (1993) conducted a characterisation study of undrained shear strength in a Holocene clay in Canada using VST data. However, they only reported the horizontal scale of fluctuation. Jaksa (1995), Jaksa, Brooker, and Kaggwa (1997) and Jaksa, Kaggwa, and Brooker (1999) reported studies of a stiff and overconsolidated Pleistocene clay at low water content, known as Keswick Clay, from Adelaide. Both the vertical and horizontal scales of fluctuation were reported based on a dense array of CPTs that is atypical in practice. Stuedlein et al. (2012) carried out a spatial variability study (δ_v and δ_h) for a desiccated Beaumont Clay (in Texas) using CPT data. Bong and Stuedlein (2017) investigated the spatial variability (δ_v and δ_h) for a beach sand in Hollywood in South California.

Nowadays, many coastal metropolises, e.g. Singapore, have completed or are planning mega reclamation projects due to the urgent need of expanding the urban area. For example, the Marina South area in Singapore

Table 2. Typical semi-variogram functions.

Model Name	Semi-variogram Function	**Scale of Fluctuation δ**
Exponential	$\gamma_{\Delta z} = C\left[1 - e^{\frac{-3\Delta z}{a}}\right] + C_0$	$\frac{2}{3}a$
Spherical	$\gamma_{\Delta z} = C\left[\frac{3\Delta z}{2a} - \frac{z\Delta z^3}{2a^3}\right] + C_0$ for $\Delta z \leq a$ $\gamma_{\Delta z} = C + C_0$ for $\Delta z \geq a$	$0.55a$
Gaussian	$\gamma_{\Delta z} = C\left[1 - e^{\frac{-3\Delta z^2}{a^2}}\right] + C_0$	a

was reclaimed on marine clay materials. Clear understanding of the spatial variability of the strength and compressibility of marine clays is important. However, in the literature, studies reporting the spatial variability of soft marine clays based on real field data have been rather limited. In this regard, a geotechnical characterisation study of the spatial variability of Singapore Kallang Formation Marine Clays using CPT data was conducted in the present study.

The estimation of scale of fluctuation can be achieved using a number of existing methods. The methods adopted in the present study include (i) Bartlett's approximation (Jaksa 1995; Jaksa, Brooker, and Kaggwa 1997; Jaksa, Kaggwa, and Brooker 1999); (ii)

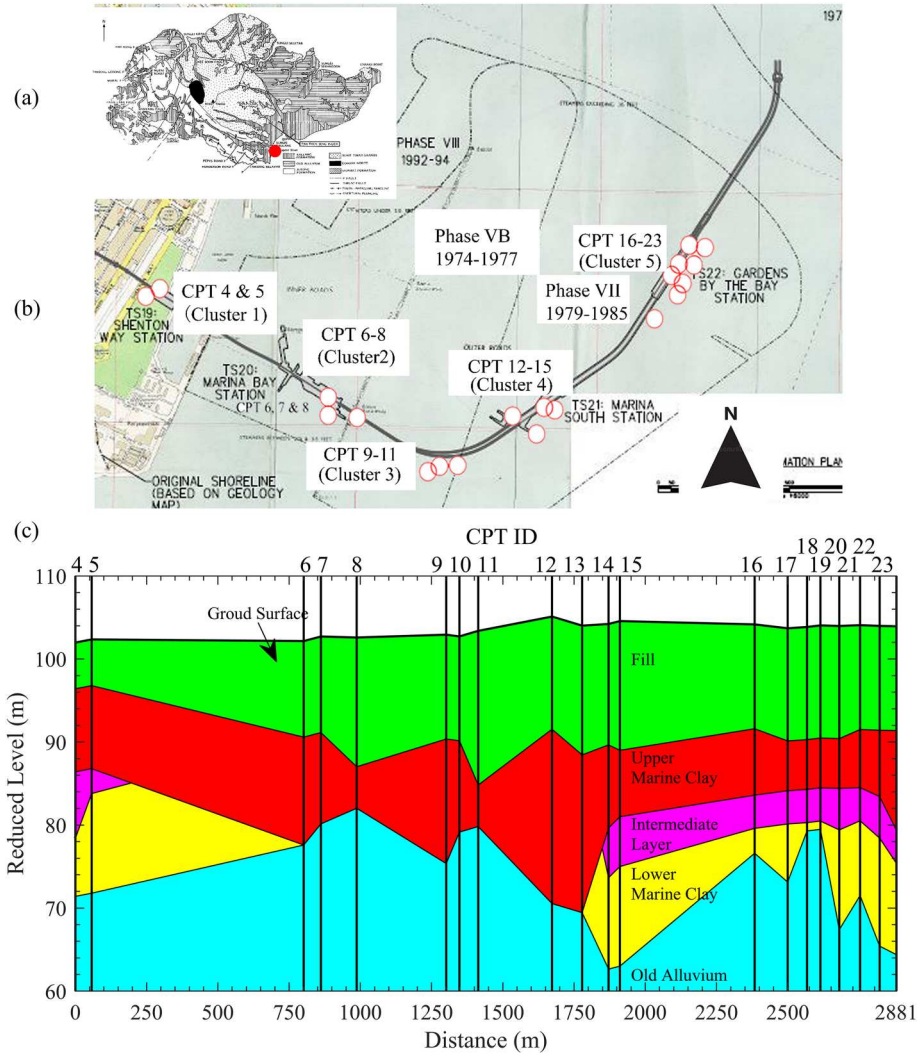

Figure 1. Overall information about the test site. (a) Location of test site in Singapore, (b) Overview of reclamation history of Marina Bay area and locations of CPTs, (c) Stratigraphy along Thomson-East Coast MRT Line.

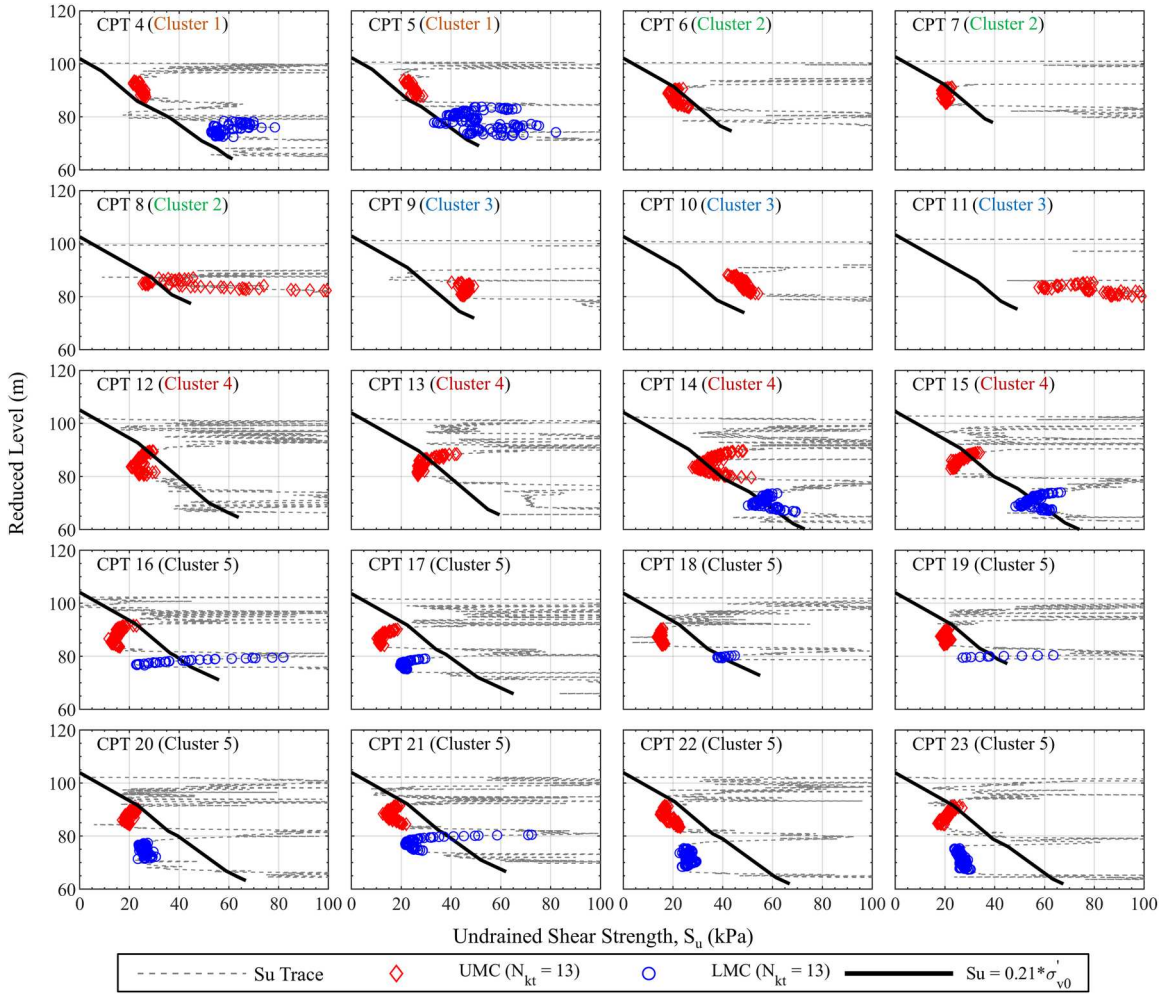

Figure 2. Undrained shear strength calculated from all 20 sets of CPT data with N_{kt} = 13.

autocorrelation or autocovariance function fitting (DeGroot and Baecher 1993; Stuedlein et al. 2012); and (iii) semi-variogram function fitting (Bong and Stuedlein 2017; Dasaka and Zhang 2012; Larsson, Stille, and Olsson 2005). Tables 1 and 2 present typical autocorrelation and semi-variogram functions reported in the literature. The single exponential (SNX), squared exponential (SQX) and second-order Markov (SOM) autocorrelation functions; and the exponential, spherical and Gaussian semi-variograms functions are considered. Some important considerations of the curve fitting exercise will be elaborated in subsequent parts of this paper.

The CPT data used in the present study were collected from different areas of Marina South in Singapore. The geological setting of this area was first described, followed by separate evaluations of the undrained shear strength, vertical scale of fluctuation and horizontal scale of fluctuation of two critical geological units in this area. The results of this study add to the database of spatial variability of natural soils and can provide useful information for reliability assessments of foundations and excavations in Marina South as well as other areas with similar geological settings.

2. Geological setting of Marina South

Figure 1(a) shows that Marina South is on central south coast of Singapore. Reclamation works at Marina South took place in three phases from 1970s to 1990s and therefore, the underlying Marine Clays have since been loaded by the reclamation fills. Figure 1(b) shows the history of the reclamation works in this area. Phase VB (1974-1977) and Phase VII (1979-1985) are of primary concern in the present study based on site investigation data obtained in these two reclaimed areas. Since the reclamation works were carried out over different period of time, the degree of consolidation of the underlying Marine Clays is believed to vary across the area.

The underlying sediments consist of the Kallang Formation and the Old Alluvium. The Kallang Formation

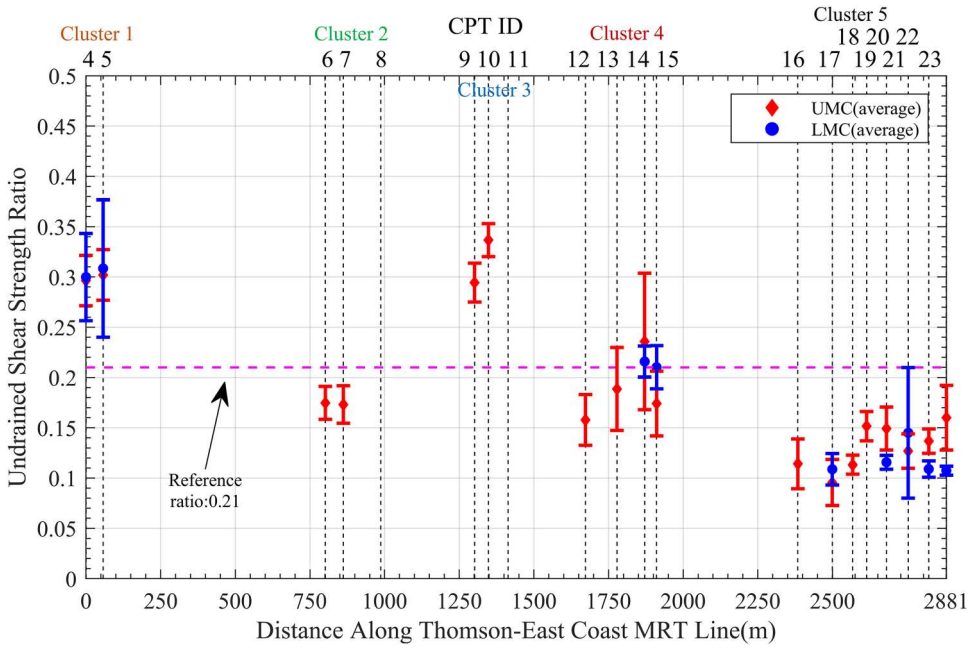

Figure 3. Undrained shear strength ratios back calculated from CPT data.

that covers most of the coastal plains and immediate offshore zones in Singapore is a recent Holocene deposit and contains soils of marine, alluvial, littoral and estuarine origins (Tan et al. 2003). Marine Clay is the most dominant geological member of the Kallang Formation and was laid down in two separate phases: the upper member known as the Upper Marine Clay (UMC) and the lower member known as the Lower Marine Clay (LMC). The LMC can be dated from approximately 12,000 years ago and the UMC was formed less than 10,000 years ago (Pitts 1992; Tan et al. 2003). These two members are often distinguished by a stiffer intermediate layer, which is considered to be the desiccated crust of the LMC when the sea level dropped approximately 10,000 years ago during the Small Ice Age.

Twenty piezocone profiles were obtained in this area as part of the site investigations for a new Mass Rapid Transit (MRT) project. Figure 1(c) shows the stratigraphy along the Thomson-East Coast MRT line. The overall thickness of the Marine Clay ranges from 10 m to 30 m. UMC unit is detected by all 20 CPTs, and LMC unit is absent from the profiles of CPTs 6 to 13. The thickness of the UMC unit varies from 10 m to 20 m while the thickness of the LMC unit ranges from 2 m to 10 m. The intermediate layer, sandwiched between UMC and LMC units, is approximately 3 m in thickness throughout the area. Old Alluvium is the dominant geological member underlying the Kallang Formation.

3. In-situ testing and characterisation of undrained shear strength

The undrained shear strength can be characterised from the net penetration resistance measurements, $q_t - \sigma_{vo}$, where q_t is the corrected cone tip resistance and σ_{vo} is the total vertical overburden stress. This is generally accomplished by assuming a cone resistance factor, N_{kt}:

$$S_u = \frac{q_t - \sigma_{vo}}{N_{kt}} \tag{1}$$

The choice of N_{kt} has been well studied for Singapore Marine Clay, with typical N_{kt} values ranging from 12 to 14 (Tan et al. 2003; Whittle and Davies 2006).

Table 3. Summary of the statistics of undrained shear strength ratio.

		Statistics of undrained shear strength ratio					
		Group 1 (Clusters 1 & 3)		Group 2 (Clusters 2 & 4)		Group 3 (Cluster 5)	
		UMC	LMC	LMC	LMC	LMC	LMC
Statistics	Mean	0.31	0.31	0.19	0.21	0.13	0.12
	COV(%)	9	20	26	9	22	28
Remarks	–	Overconsolidated		Lightly underconsolidated		Underconsolidated	

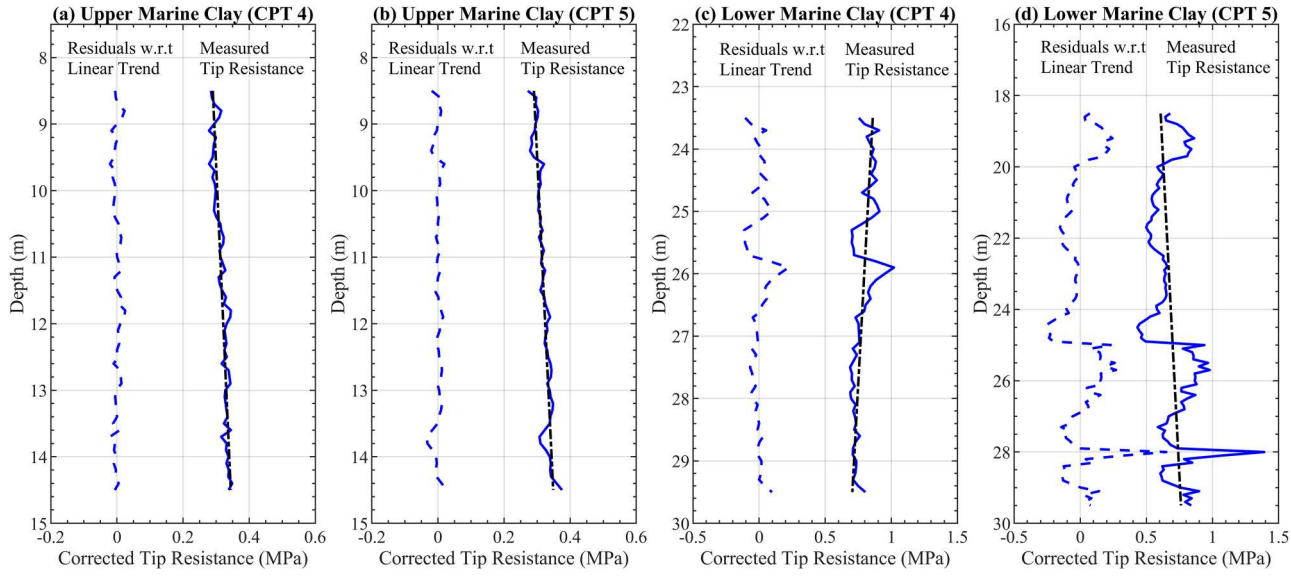

Figure 4. Examples of fitting CPT profiles with a linear trend function.

N_{kt} = 13 was chosen in the present study, and this choice is in line with the parameter adopted for excavation projects carried out in this area.

Data from 20 CPTs were considered in the present study. As indicated in Figure 1(b), these CPTs were clustered at five discrete locations in the Marina South area. Cluster 1 (CPTs 4 and 5) is located outside the reclaimed area. Clusters 2–4 (CPTs 6-15) are primarily located along south of the shoreline where the reclamation works were carried out in the 1970s while Cluster 5 (CPTs 16-23) is near to north of the shoreline where the reclamation works were completed in the 1980s.

With $N_{kt} = 13$, the undrained shear strength profiles calculated from all 20 sets of CPT data are illustrated in Figure 2. The five clusters are indicated in the figure. Reference S_u profiles deduced based on $S_u = 0.21\sigma'_{vo}$, a well-known undrained shear strength ratio of normally consolidated Singapore Marine Clay (Tan et al. 2003; Whittle and Davies 2006), are plotted in the figure for comparison purposes. The undrained shear strength profiles pertaining to UMC and LMC units are also separately highlighted along the S_u trace of the full profile from the CPTs. Data of CPTs 4 and 5, which are located outside the reclaimed area, show that the undrained shear strength profiles of UMC exhibit noticeable variations with depth (or effective overburden stress), and both UMC and LMC units from these two CPTs are observed to be lightly overconsolidated. Data of Cluster 2 (CPTs 6-8), Cluster 4 (CPTs 12-15) and Cluster 5 (CPTs 16-23) show that the undrained shear strengths of both UMC and LMC units are largely lower than the reference strength ($S_u < 0.21\sigma'_{vo}$). Assuming that the choice of N_{kt} is reasonable, the lower undrained shear strengths suggest that both units are underconsolidated under more than 10 m of reclaimed fills. However, the degrees of consolidation in Clusters 2 and 4 are slightly higher compared to Cluster 5. Data of Cluster 3 (CPTs 9-11) show that both clay units are overconsolidated although these CPTs are located in the reclaimed area. This is likely due to the presence of structures at this location prior to the reclamation works (Fan 2015).

Table 4. Results of Kendall's tau test and modified Bartlett test of all 20 sets of CPT data of UMC.

CPT ID	Kendall's τ test *p*-value	Modified Bartlett test	CPT ID	Kendall's τ test *p*-value	Modified Bartlett test
4^1	0.93(Pass)	Pass	$*14^4$	0.49(Pass)	Fail
5^1	0.91(Pass)	Fail	15^4	0.76(Pass)	Pass
6^2	0.97(Pass)	Pass	16^5	0.85(Pass)	Pass
7^2	0.70(Pass)	Pass	$*17^5$	0.98(Pass)	Pass
8^2	0.91(Pass)	Fail	18^5	0.91(Pass)	Pass
$*9^3$	0.92(Pass)	Fail	19^5	0.69(Pass)	Fail
10^3	0.85(Pass)	Pass	20^5	0.98(Pass)	Pass
11^3	0.66(Pass)	Pass	$*21^5$	0.89(Pass)	Pass
$*12^4$	0.73(Pass)	Fail	$*22^5$	0.93(Pass)	Pass
$*13^4$	0.68(Pass)	Pass	23^5	0.55(Pass)	Fail

Superscript indicates cluster ID in Figure 1(b). *with quadratic polynomial trend removed.

Table 5. Results of Kendall's tau test and modified Bartlett test of all 12 sets of CPT data of LMC.

CPT ID	Kendall's τ test *p*-value	Modified Bartlett test	CPT ID	Kendall's τ test *p*-value	Modified Bartlett test
4^1	0.39(Pass)	Pass	18^5	0.26(Pass)	Pass
5^1	0.58(Pass)	Fail	19^5	0.74(Pass)	Pass
$*14^4$	0.96(Pass)	Pass	20^5	0.90(Pass)	Pass
$*15^4$	0.94(Pass)	Pass	21^5	0.00001(Fail)	Fail
$*16^5$	0.54(Pass)	Fail	22^5	0.96(Pass)	Pass
$*17^5$	0.85(Pass)	Pass	23^5	0.59(Pass)	Pass

Superscript indicates cluster ID in Figure 1(b). *with quadratic polynomial trend removed.

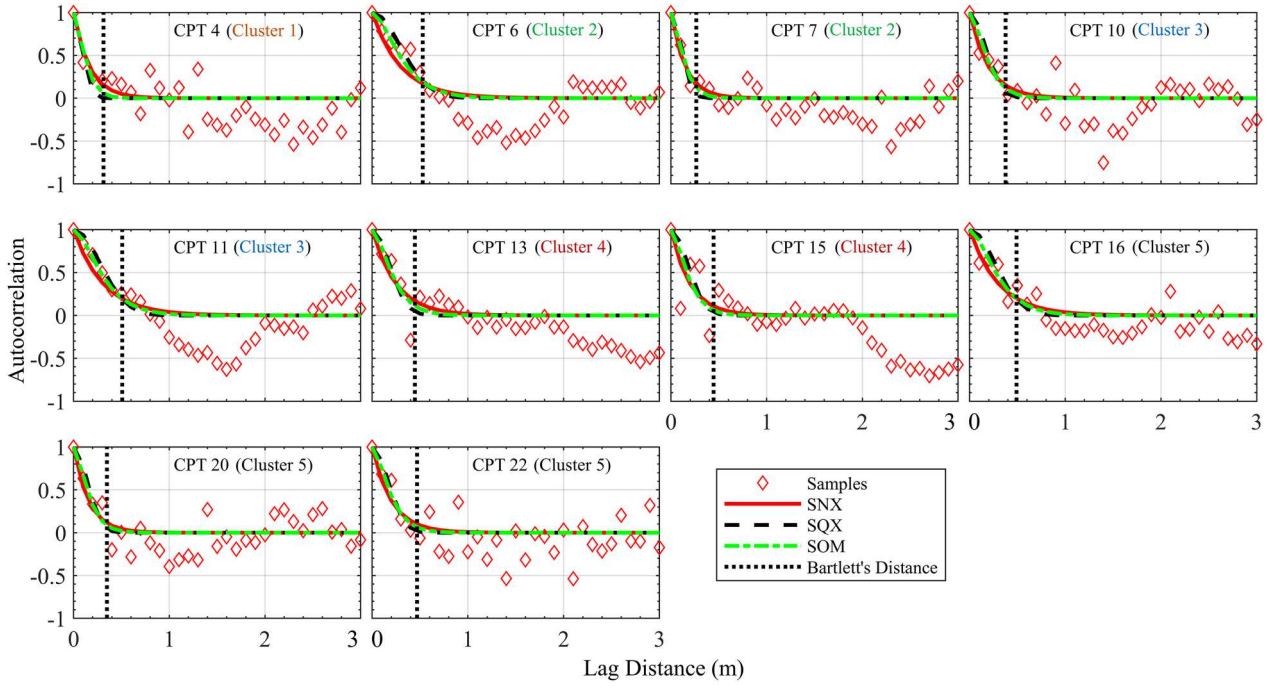

Figure 5. Results of autocorrelation model fitting (Vertical direction of UMC). Only results up to a lag distance of 3 m are shown for better visualisation.

The drainage behaviour in both clay units can be inferred from the shape of the undrained shear strength profiles shown in Figure 2. The dissipation of excessive pore water pressure closer to drainage boundaries has caused an increase in effective stress and undrained shear strength compared to soil bodies near to the middle of the clay layers, which have experienced less dissipations due to longer drainage paths. This behaviour has consequently led to the curvatures observed in most of the undrained shear strength profiles in Figure 2.

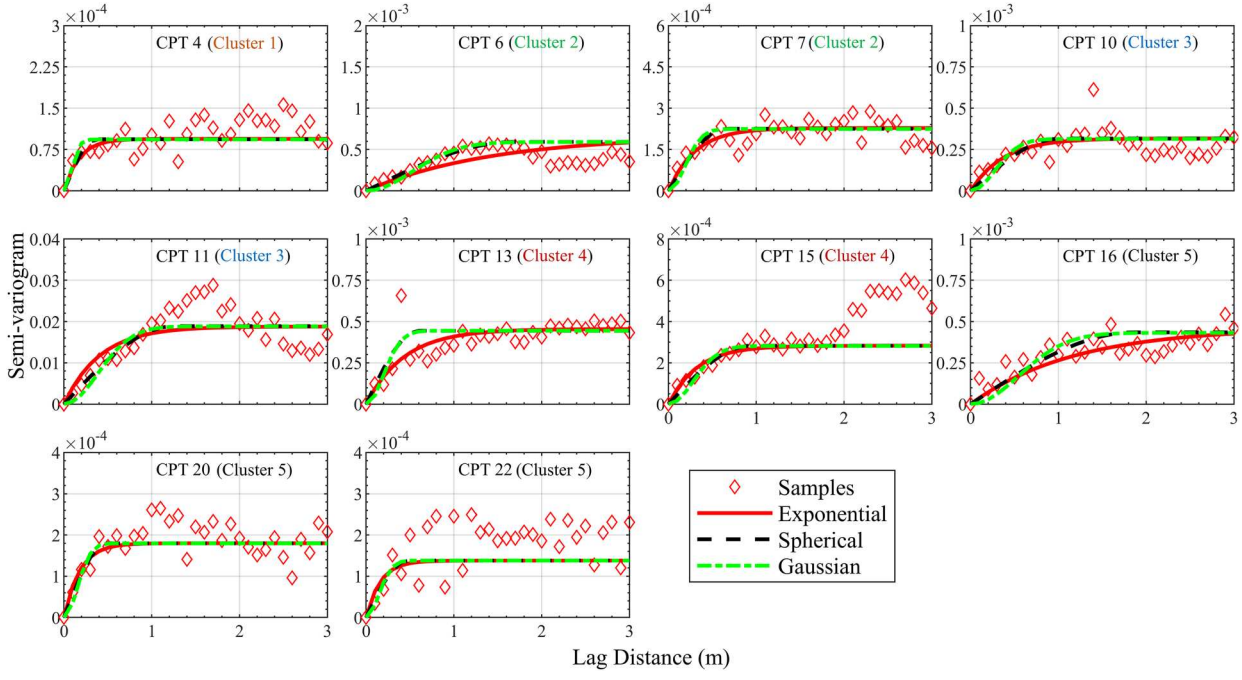

Figure 6. Results of semi-variogram model fitting (Vertical direction of UMC). Only results up to a lag distance of 3 m are shown for better visualisation.

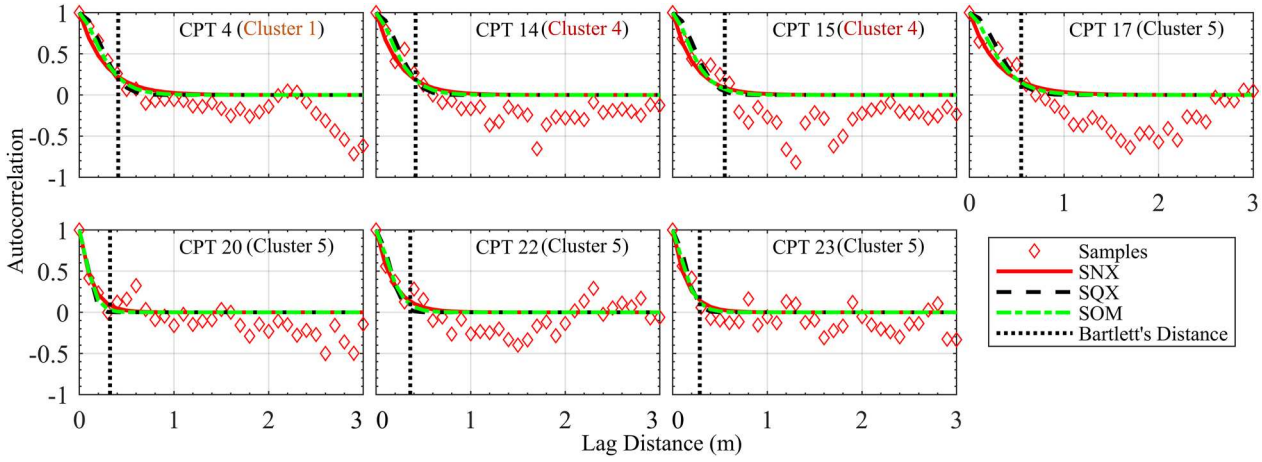

Figure 7. Results of autocorrelation model fitting (Vertical direction of LMC). Only results up to a lag distance of 3 m are shown for better visualisation.

While dissipation of the excessive pore water pressure to the overlying fills has been confirmed by almost all CPT profiles (Clusters 2, 4 and 5), the drainage behaviour to the underlying intermediate layer and Old Alluvium layer varies. Data of CPT 14, for example, strongly suggests 2-way drainage in both UMC and LMC units. In contrast, Data CPTs 20, 22 and 23, for example, strongly suggest that the intermediate layer and the Old Alluvium layer were particularly impermeable and therefore, 1-way drainage to the overlying fill layer has been the dominant behaviour at these locations. These observations suggest the complexity of drainage behaviour in these geological settings and underscore the critical needs for careful site investigations.

Figure 3 shows the back-calculated undrained shear strength ratios, $\frac{S_u}{\sigma'_{vo}}$ (Tan et al. 2003; Whittle and Davies 2006). The scatters represent the mean values while the error bars indicate one standard deviation. CPTs 8 and 11 were excluded for the study of UMC units due to the large variations. According to Figure 1(c), thin crusts of LMC are surveyed by CPTs 16, 18 and 19. The insertion of a piezocone, which creates a stress bulk that may extend beyond the LMC unit, may not produce tip resistances that are representative of the LMC units at these locations. Therefore, CPTs 16, 18 and 19 were excluded for the study of LMC units.

Results of CPTs 4 and 5 indicate that the undrained shear strength ratios are similar between UMC and LMC units. Based on $\frac{Su}{\sigma'_{vo}} = 0.21 \times OCR^m$, a well-known undrained shear strength ratio of overconsolidated Singapore Marine Clay, an undrained shear strength ratio $(\frac{Su}{\sigma'_{vo}})$ of 0.3 corresponds to an overconsolidation ratio of approximately 1.56 with a typical power coefficient m of 0.8 (D'Ignazio et al. 2016). CPTs 6 and 7 (Cluster 2) and CPTs 12-15 (Cluster 4) show similar values of undrained shear strength ratio although more significant variations are observed in CPTs 13-15 (Cluster 4). Cluster 5 that consists of CPTs 16-23 shows relatively lower values of undrained shear strength ratio as compared to Clusters 2 and 4 for both UMC and LMC units.

Based on the results shown in Figures 2 and 3, it is possible to broadly classify the data into three groups. The first group contains CPTs in Clusters 1 and 3. This group pertains to clay units that are overconsolidated. CPTs in Clusters 2 and 4 belong to Group 2 while CPTs in Cluster 5 are in Group 3 because a relatively higher degree of consolidation was observed in Clusters 2 and 4. This grouping is also in line with the reclamation history shown in Figure 1(b), where Clusters 2 and 4 are largely within Phase VB (1970s) and Cluster 5 is within Phase VII (1980s). Based on this grouping, the statistics of the undrained shear strength ratio are tabulated in Table 3. It is worth noting that the statistics of the undrained shear strength ratio involve both aleatory and epistemic components. The inherent variability in the undrained shear strength ratio along the depth, captured by the standard deviation, primarily reflects aleatory uncertainty due to the natural randomness in soil properties. However, the process of estimating this variability from a finite number of samples introduces epistemic uncertainty, as the precision of the estimate depends on the sample size. In the present study, there is a relatively large amount of data for estimating the standard deviation of the undrained shear strength ratio, given the small vertical interval of CPT measurements (0.1 m). Therefore, the uncertainty addressed here is mainly aleatory but

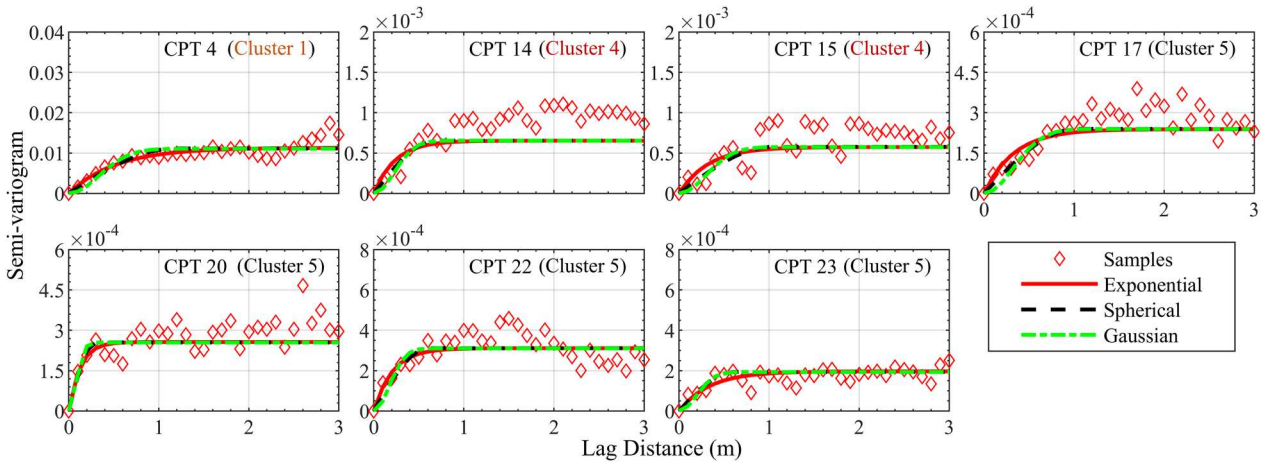

Figure 8. Results of semi-variogram model fitting (Vertical direction of LMC). Only results up to a lag distance of 3 m are shown for better visualisation.

contains a small component of epistemic uncertainty. Results show that the undrained shear strength ratios are largely similar between UMC and LMC units across the three groups, and the mean ratios of group 2 are significantly larger than those of group 3. The COVs, 9–28%, suggest that moderate uncertainties are associated with the undrained shear strength ratios of the two soil units.

4. Vertical scale of fluctuation

A prerequisite for the characterisation of spatial variability is the conditioning of data to achieve weak stationarity (Hu and Wang 2024; Jaksa, Kaggwa, and Brooker 1999; Phoon, Quek, and An 2003). A profile of measurement of interest is said to be weakly stationary if: (i) the mean is constant; and (ii) the autocovariance is only a function of the distance between observations (Phoon, Quek, and An 2003). The first condition can be approximately achieved by removing the trend function. A linear trend function is often sufficient although the use of a quadratic polynomial trend function has also been reported in the literature (Jaksa 1995; Jaksa, Brooker, and Kaggwa 1997; Jaksa, Kaggwa, and Brooker 1999). It is worth mentioning that a trend function with a minimum order is preferred as over-fitting may result in inaccurate estimation of scale of fluctuation. Figure 4 shows selected CPT profiles and the corresponding residual profiles with a linear trend function. Although a linear trend function appears to be sufficient, further statistical assessments are needed to test the adequacy of the trend function and the quality of the residuals. Various techniques can be used to assess stationarity. Kendall's tau test (Jaksa 1995; Jaksa, Brooker, and Kaggwa 1997; Jaksa, Kaggwa, and Brooker 1999; Sen 1968) and modified Bartlett test (MBS) (Phoon, Quek, and An 2003; Phoon, Quek, and An 2004) were adopted in the present study.

Table 6. Summary of vertical scale of fluctuation of UMC using CPT data.

			Scale of Fluctuation (*m*)						
			Autocorrelation Function			Semi-variogram Function			-
CPT ID	State of Consolidation	Number of Data	SNX	SQX	SOM	Exponential	Spherical	Gaussian	Bartlett's distance
4^1	Overconsolidated	61	0.33	0.22	0.27	0.35	0.2	0.21	0.31
6^2	Lightly Underconsosolidated	71	0.6	0.74	0.68	2.89	0.93	1.29	0.53
7^2	Lightly Underconsosolidated	61	0.3	0.27	0.29	0.61	0.35	0.46	0.26
10^3	Overconsolidated	71	0.4	0.41	0.41	0.75	0.55	0.68	0.38
11^3	Overconsolidated	71	0.62	0.7	0.67	0.83	0.69	0.95	0.51
13^4	Lightly Underconsosolidated	81	0.5	0.45	0.48	0.87	0.33	0.48	0.45
15^4	Lightly Underconsosolidated	61	0.4	0.44	0.39	0.66	0.51	0.69	0.44
16^5	Underconsosolidated	81	0.61	0.67	0.65	2.36	1.02	1.34	0.49
20^5	Underconsosolidated	61	0.32	0.35	0.34	0.36	0.27	0.37	0.35
22^5	Underconsosolidated	81	0.41	0.42	0.42	0.33	0.26	0.35	0.47
Mean (m)			0.45	0.47	0.46	0.99	0.51	0.68	0.42
Standard Deviation (m)			0.12	0.18	0.16	0.89	0.29	0.39	0.09
COV(%)			28	38	34	89	57	57	21

Superscript indicates cluster ID in Figure 1(b)

Table 7. Summary of vertical scale of fluctuation of LMC using CPT data.

			Scale of Fluctuation (m)						
			Autocorrelation Function			Semi-variogram Function			-
CPT ID	State of Consolidation	Number of Data	SNX	SQX	SOM	Exponential	Spherical	Gaussian	Bartlett's distance
4^1	Overconsolidated	71	0.54	0.57	0.57	1.05	0.65	0.82	0.41
14^4	Lightly Underconsosolidated	81	0.49	0.56	0.53	0.48	0.37	0.55	0.42
15^4	Lightly Underconsosolidated	81	0.45	0.54	0.51	0.65	0.57	0.74	0.55
17^5	Underconsosolidated	51	0.60	0.69	0.65	0.67	0.56	0.80	0.55
20^5	Underconsosolidated	51	0.26	0.21	0.23	0.25	0.16	0.20	0.32
22^5	Underconsosolidated	81	0.36	0.33	0.36	0.41	0.33	0.42	0.36
23^5	Underconsosolidated	91	0.30	0.32	0.31	0.68	0.33	0.47	0.29
Mean (m)			0.43	0.46	0.45	0.60	0.42	0.57	0.41
Standard Deviation (m)			0.13	0.17	0.15	0.25	0.17	0.23	0.10
COV(%)			30	37	34	43	41	40	25

Superscript indicates cluster ID in Figure 1(b)

Tables 4 and 5 present the results of the statistical assessments for UMC and LMC respectively. UMC is detected by all 20 sets of CPTs while LMC is only observed in 12 sets of CPTs. Superscripts in both tables indicate the cluster ID shown in Figure 1(b). A linear trend is not always sufficient and therefore, a quadratic polynomial trend was used for some CPTs, which are labelled in both tables. Results show that 13 sets of CPTs pertaining to UMC passed both statistical assessments and therefore, they are deemed sufficiently homogeneous for subsequent characterisation exercises. Pertaining to LMC, 9 out of 12 sets of CPTs passed both statistical assessments. As a result, the subsequent analyses are carried out based on these CPTs that passed both tests.

Autocorrelation function fitting, semi-variogram function fitting and Bartlett's approximation were adopted to characterise the vertical scale of fluctuation. All data points of the CPTs that passed the statistical assessments were sampled with a vertical interval of 0.1 m. The analysis starts from evaluating sample autocorrelation coefficient $\rho_{\Delta z}$ and sample semi-variogram value $\gamma_{\Delta z}$ of all lag distances. At a lag distance Δz, the corresponding sample autocorrelation coefficient $\rho_{\Delta z}$ and sample semi-variogram value $\gamma_{\Delta z}$ can be evaluated as follows:

$$\rho_{\Delta z} = \frac{\sum_{i=1}^{N(\Delta z)} \frac{(q_{t,\,i+\Delta z} - \mu_{q_{t,\,i+\Delta z}})}{\sigma_{q_{t,\,i+\Delta z}}} \frac{(q_{t,\,i} - \mu_{q_{t,\,i}})}{\sigma_{q_{t,\,i}}}}{N(\Delta z)\text{-}1} \quad (2)$$

$$\gamma_{\Delta z} = \frac{\sum_{i=1}^{N(\Delta z)} (q_{t,\,i+\Delta z} - q_{t,\,i})^2}{2N(\Delta z)} \quad (3)$$

where $\rho_{\Delta z}$ and $\gamma_{\Delta z}$ are the autocorrelation coefficient and semi-variogram value respectively at lag distance Δz; $q_{t,\,i+\Delta z}$ and $q_{t,\,i}$ are the corrected cone tip resistance pairs separated by the lag distance Δz; $\mu_{q_{t,\,i+\Delta z}}$, $\sigma_{q_{t,\,i+\Delta z}}$, $\mu_{q_{t,\,i}}$ and $\sigma_{q_{t,\,i}}$ are the mean and standard deviation of $q_{t,\,i+\Delta z}$ and $q_{t,\,i}$; and $N(\Delta z)$ is the total number of data pairs separated by a lag distance Δz.

Figures 5–8 summarize the sample autocorrelation coefficients and semi-variogram values as functions of lag distances for UMC and LMC units. The cluster (as per in Figure 1(b)) that the CPTs belong to has been highlighted. The autocorrelation coefficients fluctuate around zero with increasing lag distances, while the semi-variogram values fluctuate around the sill. These patterns confirm weak stationarity in the data (Box et al. 2015; Davis and Sampson 1986), and support the order of the trend functions used.

The autocorrelation functions and semi-variogram functions listed in Tables 1 and 2 are used to fit to the samples using the ordinary least square method. It should be noted that the curve fitting exercise involved truncation of the lag distances due to decreasing reliability of widely separated distance (Jaksa, Kaggwa, and Brooker 1999; Oguz, Huvaj, and Griffiths 2019; Uzielli, Vannucchi, and Phoon 2005). In the current study, following the recommendation of Lumb (1974) and Spry, Kulhawy, and Grigoriu (1988), the first quarter of lag distances, which correspond to lag distances up to approximately 1.5 m, were used to fit the functions. Pertaining to fitting of semi-variogram functions, zero nugget was assumed. In the present study, all CPTs were performed by an established site investigation contractor in Singapore following standardized operation procedures with well-maintained equipment. As a result, it is reasonable to assume that the effect of measurements error is minor, and it is reasonable to assume a zero nugget.

The Bartlett's approximation, a commonly used technique in the field of time series analysis, is different from the fitting of autocorrelation functions in the sense that no assumed functions are needed. A Bartlett's limit is a threshold autocorrelation coefficient that can be computed using Equation (4). The lag distance corresponding to the intersection of the sample autocorrelation

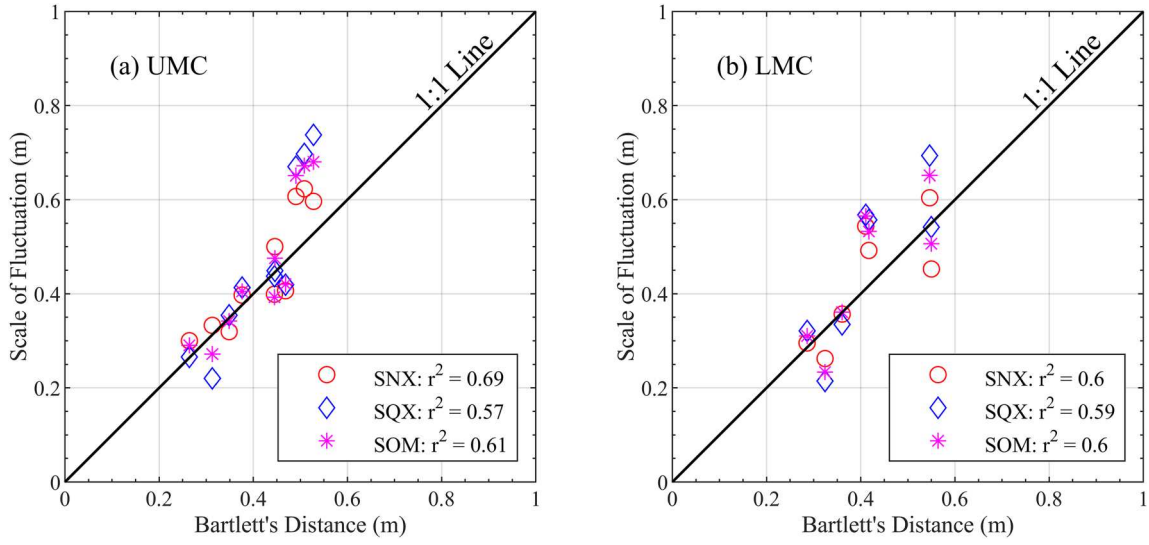

Figure 9. Comparison of Bartlett's distance with scale of fluctuation derived from fitting of autocorrelation functions.

coefficients and the Bartlett's limit is, therefore, termed as Bartlett's distance (Jaksa 1995).

$$r_B = \frac{1.96}{\sqrt{n}} \tag{4}$$

where n is the total number of lag distances.

The results of the curve fitting exercise and the Bartlett's distances are shown in Figures 5–8. It should be noted that some CPTs have been removed, although these CPTs passed both statistical tests. CPTs 17, 18 and 21 were removed for the study of UMC, and CPTs 18 and 19 were removed for the study of LMC. The scales of fluctuation derived from these CPTs were of comparable magnitudes of the CPT sampling interval (0.1 m) and thus being less meaningful (Huber 2013; Oguz, Huvaj, and Griffiths 2019).

Tables 6 and 7 summarise the results of the computed vertical scales of fluctuation for UMC and LMC units. The cluster that each CPT belongs to is indicated by the superscript. It is important to note that there is no noticeable trend in the values of δ_v across clusters for both UMC and LMC units. This suggests that the degree of consolidation has had limited influence on the values of δ_v, given that Clusters 1 and 3 are characterised by overconsolidated soils, Clusters 2 and 4 with lightly underconsolidated soils, and Cluster 5 with underconsolidated soils. The three autocorrelation functions estimate a mean value of $\delta_v = 0.45$ m and a COV of 33% for the UMC while the three semi-variogram functions predict a larger mean value of $\delta_v = 0.73$ m and a larger COV of 67%. The vertical scale of fluctuation is similar to LMC. The mean values of $\delta_v = 0.45 \pm 0.15$ m and $\delta_v = 0.73 \pm 0.52$ m for the autocorrelation functions and semi-variogram functions respectively. In general, the exponential and Gaussian semi-variogram functions produce slightly larger values of δ_v compared to the three autocorrelation functions while spherical semi-variogram function yield comparable results.

Table 8. Summary of horizontal scale of fluctuation of UMC using CPT data.

	Scale of Fluctuation (*m*)					
	Autocorrelation Function			Semi-variogram Function		
Reduced Level, RL (m)	SNX	SQX	SOM	Exponential	Spherical	Gaussian
89.3	113.2	133.5	121.2	135.5	102.2	138.3
88.8	127.2	139.3	130.8	150.6	108.9	145.0
88.3	129.4	134.9	128.8	165.4	114.9	151.0
87.8	114.8	120.7	115.6	160.2	107.5	142.9
87.3	101.0	104.8	101.2	162.7	114.4	139.4
86.8	149.0	145.0	142.0	202.5	159.0	193.3
86.3	157.8	156.9	154.0	189.3	162.2	199.6
85.8	165.0	160.9	158.4	224.2	184.5	236.1
84.3	132.2	137.4	132.0	189.3	189.4	196.6
Mean (m)	132.2	137.0	131.6	175.5	138.1	171.4
Standard Deviation (m)	21.5	17.2	18.1	27.8	35.3	35.6
COV(%)	16	13	14	16	26	21

Table 9. Summary of horizontal scale of fluctuation of LMC using CPT data.

	Scale of Fluctuation (*m*)					
	Autocorrelation Function			Semi-variogram Function		
Reduced Level, RL (m)	SNX	SQX	SOM	Exponential	Spherical	Gaussian
77.4	158.8	142.0	155.6	177.8	129.3	163.3
76.9	121.8	131.2	128.8	201.8	191.2	208.6
76.4	126.0	138.8	136.4	182.1	121.5	174.6
75.9	98.2	123.9	109.2	147.5	95.8	149.0
75.4	90.2	118.4	101.6	110.4	80.9	127.8
Mean (m)	119.0	130.8	126.3	163.9	123.7	164.7
Standard Deviation (m)	26.9	9.9	21.6	35.7	42.4	30.2
COV(%)	23	8	17	22	34	18

The Bartlett's approximation yields mean values of $\delta_v = 0.42$ m and $\delta_v = 0.41$ m for UMC and LMC units. These values are very similar to the results of the three autocorrelation functions. However, the Bartlett's approximation yields smaller values of COVs (21% and 25% for UMC and LMC respectively) compared to the three autocorrelation and semi-variogram functions. Figure 9 compares Bartlett's distances with scales of fluctuation derived from fitting of autocorrelation functions. The values of coefficients of determination indicate that there is a moderately strong correlation between the two sets of scales of fluctuation. This observation is consistent with results reported by Jaksa (1995).

5. Horizontal scale of fluctuation

The characterisation of horizontal scale of fluctuation is more challenging and has not been reported frequently in the literature. In the present study, the horizontal scale of fluctuation was characterised by fitting autocorrelation and semi-variogram functions. Following the existing literature (Bong and Stuedlein 2017; Jaksa 1995; Stuedlein et al. 2012), UMC and LMC layers were subdivided into a series of horizontal slices, each 0.5 m in thickness. Tables 8 and 9 show the elevations, represented by reduced level (RL), of all slices considered in the present study. The horizontal scale of fluctuation was separately characterised for each slice. In addition, the horizontal lag distance between any two CPT locations was taken as the Euclidean distance (i.e. smallest lag distance is approximately 40 m). Such a configuration effectively simplifies the 2-D problem into a 1-D problem. The omission of directional variations in deriving the horizontal scale of fluctuation is believed to align with geological settings in marine clays, and similar simplifications have also been reported by Stuedlein et al. (2012) and Bong and Stuedlein (2017). In the present study, there are 20 and 12 CPT locations for UMC and LMC respectively. As a result, there exist 190 and 66 lag distance values ($190 = C_2^{20}$; $66 = C_2^{12}$) for UMC and LMC respectively. Weak stationarity is believed to be achieved for each slice by removing a linear surface-polynomial trend function (DeGroot and Baecher 1993). Residuals with respect to this trend were then used to evaluate autocorrelation coefficients and semi-variogram values following Equations (2) and (3).

It is worth mentioning that a sufficiently large value of $N(\Delta z)$, which corresponds to the number of CPT data pair, is desirable and necessary for meaningful evaluations of $\rho_{\Delta z}$ and $\gamma_{\Delta z}$ for each lag distance Δz. However, given a slice thickness of 0.5 m and a CPT sampling interval of 0.1 m, N = 5 can be obtained for each lag distance Δz, which is likely to be insufficient. Therefore, it is proposed to group lag distances so that there are sufficient CPT data pairs for the evaluation of $\rho_{\Delta z}$ and $\gamma_{\Delta z}$.

Lag distances are first organised in an ascending order. The corrected cone tip resistances of similar lag distances are then combined to form a larger data set for the evaluation of $\rho_{\Delta z}$ and $\gamma_{\Delta z}$ of the group. Taking the data at RL = 89.3 m as the example (Figure 10), the first few ungrouped lag distances available are 40, 43, 46, 47 and 49 m. Each lag distance contains 5 data pairs of corrected cone tip resistances. These five lag distances are then combined to form a larger group that contains 25 CPT data pairs. The lag distance of this group is represented by the mean of these five lag distance values (45 m), and the value of autocorrelation coefficient (ρ_{45}) is evaluated as −0.08 based on these 25 CPT data pairs. Therefore, this coordinate, (45, −0.08), is then plotted as the second sample autocorrelation coefficient scatter with the first scatter being (0, 1) in the first subplot in Figure 10. The autocorrelation coefficients and semi-variogram values at other lag distance groups and reduced levels (elevations) can then be computed in a similar manner, and the results are summarized in Figures 10–13. Similar technique was adopted by DeGroot and Baecher (1993) to smooth sparse data, but details were not described in the study. The clustering technique used in the present

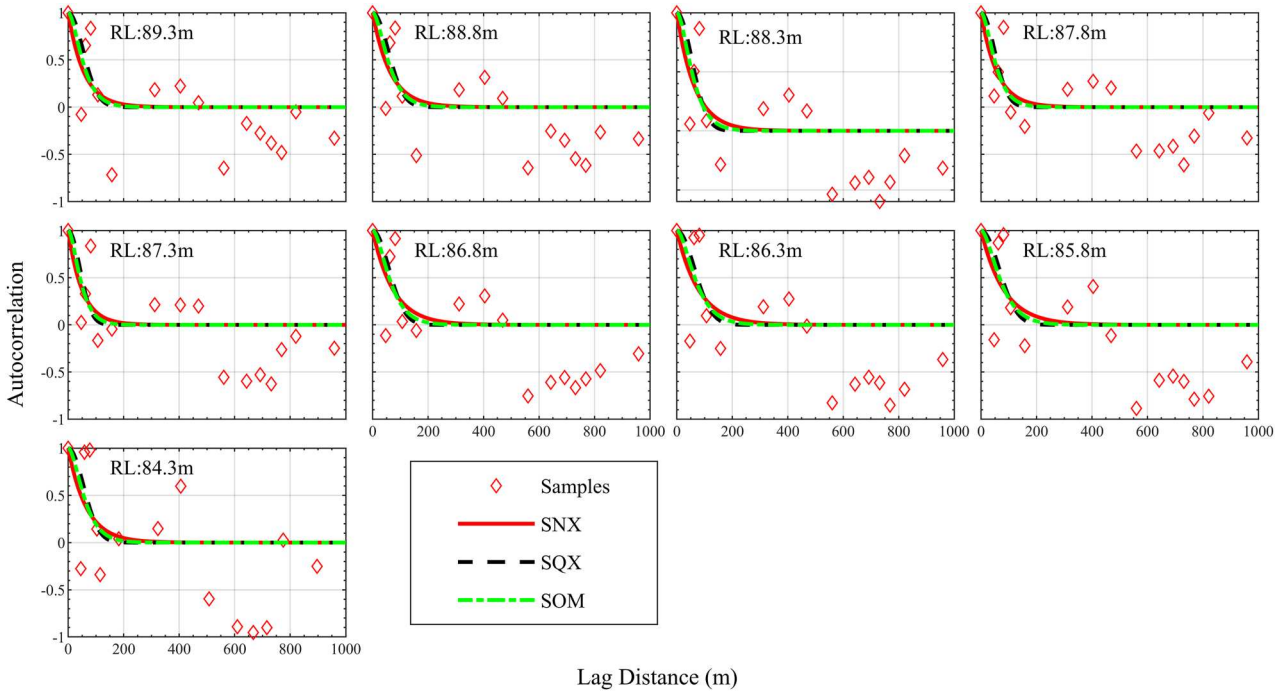

Figure 10. Results of autocorrelation model fitting (Horizontal direction of UMC).

study is believed to be a reasonable interpretation of the technique used by DeGroot and Baecher (1993). It is worth noting that the estimation of autocorrelation coefficients and semi-variogram values in the horizontal direction can be a challenging task, especially when there are limited site investigation data. Most importantly, the determination of scale of fluctuation may be sensitive to the smallest lag distance. Following the configuration described above, there can be a trade-off between the number of CPT data pairs and the resolution of lag distance. On the one hand, averaging over more lag distances could

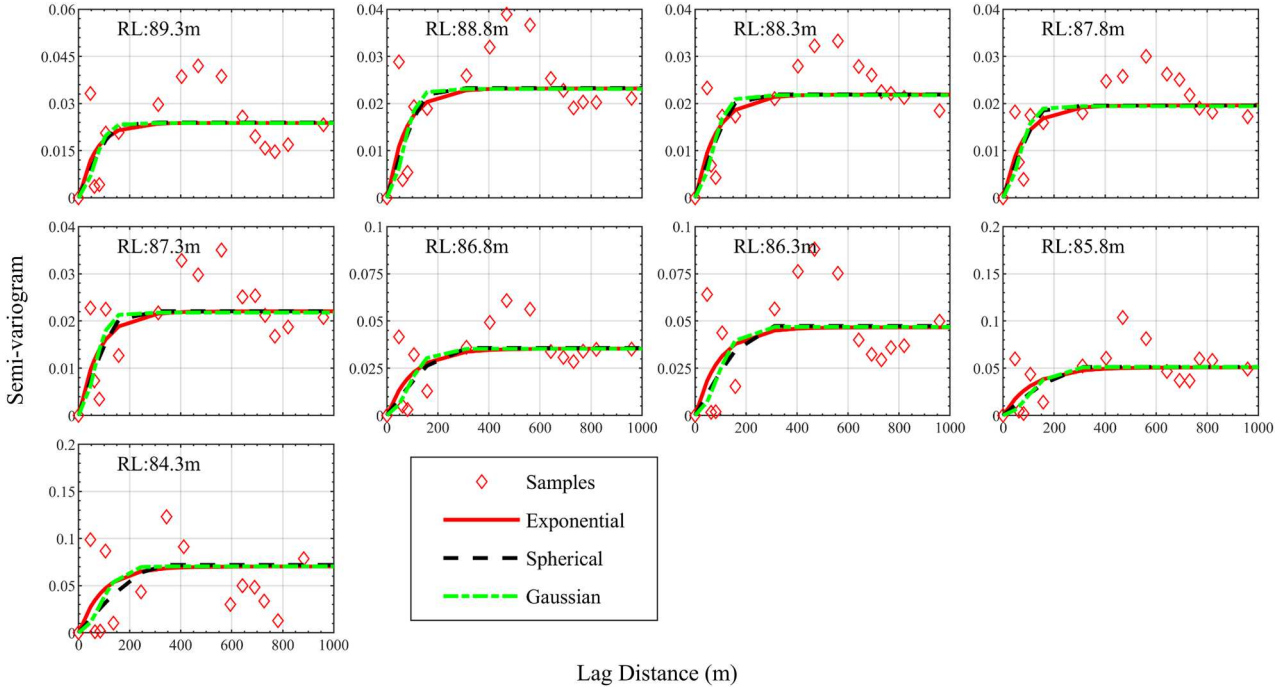

Figure 11. Results of semi-variogram model fitting (Horizontal direction of UMC).

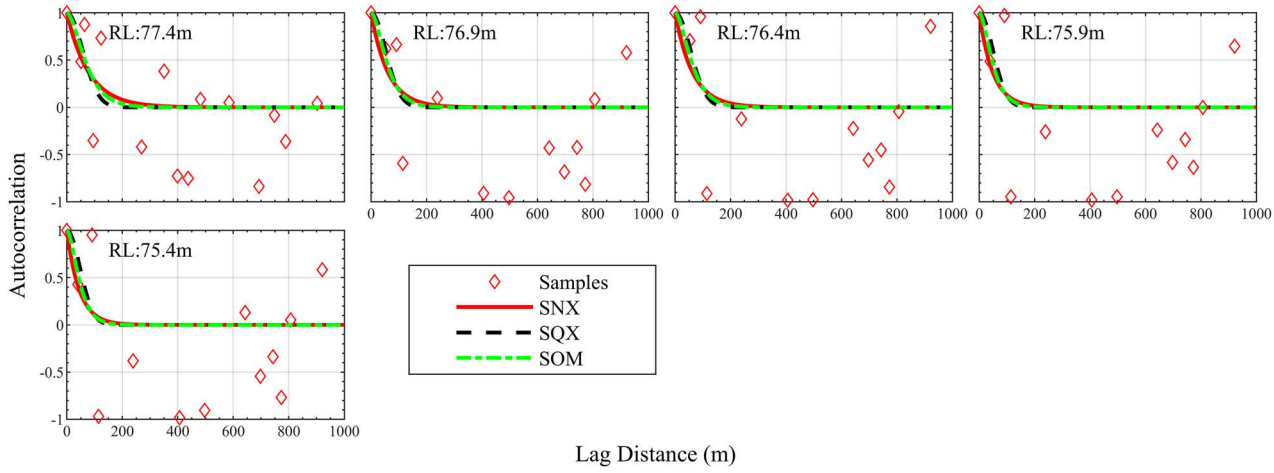

Figure 12. Results of autocorrelation model fitting (Horizontal direction of LMC).

increase the number of CPT data pairs within a lag distance group. On the other hand, increasing the resolution of lag distance would reduce the number of CPT data pairs within a lag distance group. In the present study, the number of CPT data pairs within a lag distance group varies. The average number of data pairs across all lag distance groups is 40, with a minimum of 24 data pairs and very few cases failing under 30. A trial-and-error exercise was experimented to arrive at this configuration, which is believed to be a balanced solution for the present study. In addition, this configuration essentially meets the 30 data pairs suggested by Journel and Huijbregts (1976) and yields fairly reliable results.

Figures 10–13 summarise the sample autocorrelation coefficients and semi-variogram values as functions of lag distances for UMC and LMC units. Globally, the data of LMC is sparser than that of UMC. According to Figure 1(c), 20 CPTs were used to characterise δ_h of UMC, while 12 CPTs were used for LMC. As a result, more information has been available for the study of UMC, which contributed to improved data quality. In general, the patterns that the autocorrelation coefficients fluctuate around zero with increasing lag distances for the study of δ_h at all reduced levels (Figures 10 and 12) are not as clear as those for the study of δ_v (Figures 5 and 7). The autocorrelation coefficients at large lag distances in Figures 10 and 12 are consistently of negative values. However, the patterns that the semi-variogram values fluctuate around the sill (Figures 11 and 13) are fairly prominent, which may suggest that the patterns shown in Figures 10 and 12 are not necessarily signs of non-stationarity, and that the use of linear surface-polynomial trend function appears to be adequate.

Tables 8 and 9 summarise the results in the computed horizontal scales of fluctuation for UMC and LMC units. In general, the exponential and Gaussian semi-variogram functions produce slightly larger values of δ_h compared to the three autocorrelation functions while spherical semi-variogram function yields comparable results. The three autocorrelation functions estimate a mean value of $\delta_h = 134$ m and a COV of 14% for UMC while the three semi-variogram functions predict a larger mean value of $\delta_h = 160$ m and a larger COV of 21%. The scale of fluctuation is slightly smaller for LMC. The mean values of $\delta_h = 125 \pm 20$ m and $\delta_h = 150 \pm 36$ m for the autocorrelation functions and semi-variogram functions, respectively.

In contrast to the results of vertical scale of fluctuation, which are of rather significant uncertainties, the uncertainties associated with horizontal scales of fluctuation are not as significant. The overall values of COVs for δ_h are approximately 18% and 20% for UMC and LMC respectively. Moreover, for both UMC and LMC, there is no noticeable trend between elevation (RL) and the magnitude of horizontal scale of fluctuation.

To further assess the credibility of the values obtained, analysis using field vane shear tests data were also carried out following the same clustering procedure and considerations aforementioned. In contrast to CPT data, VST data were sampled much more coarsely in the vertical direction and therefore, a group size of nine was used to ensure that autocorrelation coefficients and semi-variogram values could be reasonably computed. Table 10 summarises the results in the computed horizontal scales of fluctuation for UMC and LMC units at selected elevations. The three autocorrelation functions estimate a mean value of $\delta_h = 138$ m for the UMC while the three semi-variogram functions predicted a mean value of $\delta_h = 128$ m. The mean values of $\delta_h = 156$ m and $\delta_h = 146$ m for the autocorrelation functions and semi-variogram functions respectively were obtained for LMC. The horizontal scales

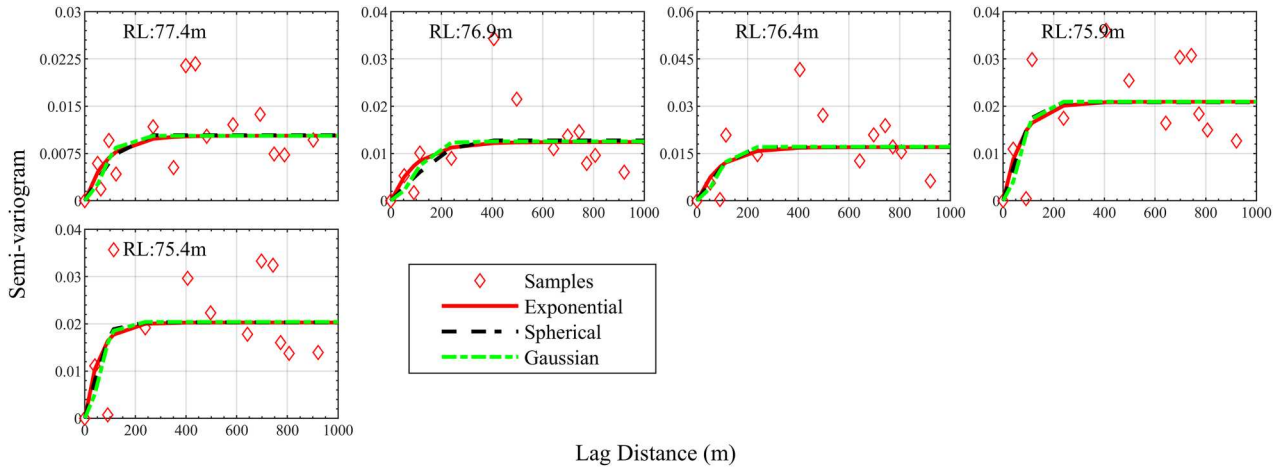

Figure 13. Results of semi-variogram model fitting (Horizontal direction of LMC).

of fluctuation derived using VST data agree reasonably well with the results obtained using CPT data for both UMC and LMC units.

6. Discussions

As highlighted in Phoon and Kulhawy (1999), the measurement error and the transformation uncertainty are another two critical sources of geotechnical uncertainty, in addition to the inherent variability. In random field or geostatistical modelling using semi-variograms, the nugget value represents the variogram value at zero or near-zero lag distance, which is typically indicative of measurement error. In the present study, the semi-variograms are computed with the assumption of a zero nugget. Tables 11 and 12 tabulate the results obtained when the nugget is considered as a fitting parameter in the semi-variogram model. The nugget-to-sill ratios, which reflect the proportion of measurement uncertainty relative to total uncertainty, are also summarised in the tables. The additional analyses suggest that that the nugget effect is not significant. Moreover, in the current study, the transformation uncertainty primarily arises from the cone factor N_{kt} = 13 used in Equation (1). In Singapore, this cone factor has been well calibrated and adopted in engineering practices (Tan et al. 2003; Whittle and Davies 2006). Therefore, low transformation uncertainty is reasonably assumed.

First, the scale of fluctuation (SoF) values, whether calculated with or without considering the nugget, are broadly comparable across all cases, with differences of approximately 10%. The nugget-to-sill ratios are largely within 10% in most cases, although some instances exceed 20%. In general, the nugget-to-sill ratios associated with vertical SoF are lower than those for horizontal SoF. This is not unexpected because the readings used for calculating vertical SoF are from the same profile, while the readings used for calculating horizontal SoF span multiple profiles which are likely associated with larger measurement errors. Furthermore, it is also observed that the Gaussian semi-variogram is more sensitive to the nugget effect, as evidenced by the relatively higher nugget-to-sill ratios compared to the other two semi-variograms. While the nugget-to-sill ratios generally indicate that the nugget effect is not dominating in the present study and most total variability is attributed to inherent spatial variability, it is recommended in practice to closely examine the nugget value to ensure that the calculated spatial variability is not masked by significant measurement errors.

Table 10. Summary of horizontal scale of fluctuation of UMC and LMC using field vane shear test data.

		Scale of Fluctuation (*m*)					
		Autocorrelation Function			Semi-variogram Function		
	Reduced Level (m)	SNX	SQX	SOM	Exponential	Spherical	Gaussian
UMC	90.3	168.0	141.3	165.2	-	-	-
	89.8	118.6	102.8	111.2	142.7	125.3	120.8
	89.3	149.0	192.8	154.8	146.4	126.9	103.0
	Mean (m)	133.8	147.8	133.0	144.6	126.1	111.9
LMC	74.5	155.8	171.0	154.8	150.9	121.9	163.3
	73.5	150.0	156.3	149.2	154.0	121.5	169.4
	Mean (m)	152.9	163.7	152.0	152.4	121.7	166.4

Table 11. Summary of results of vertical scale of fluctuation of UMC and LMC considering nugget.

	Exponential				Spherical				Gaussian			
	SoF (*m*)		Nugget/Sill		SoF (*m*)		Nugget/Sill		SoF (*m*)		Nugget/Sill	
CPTID	UMC	LMC	UMC	LMC	UMC	LMC	UMC	LMC	UMC	LMC	UMC	LMC
4	0.23	0.79	10.1%	4.7%	0.21	0.66	10.0%	5.9%	0.21	0.93	3.3%	14.1%
6	2.49	–	11.5%	–	0.78	–	7.5%	–	1.39	–	13.4%	–
7	0.58	–	8.0%	–	0.28	–	8.1%	–	0.51	–	18.9%	–
10	0.76	–	8.3%	–	0.43	–	9.9%	–	0.78	–	24.1%	–
11	0.82	–	1.0%	–	0.69	–	1.2%	–	1.01	–	11.8%	–
13	0.79	–	7.6%	–	0.35	–	8.9%	–	0.49	–	3.5%	–
14	–	0.53	–	5.6%	–	0.36	–	8.6%	–	0.54	–	6.3%
15	0.72	0.68	7.8%	6.1%	0.43	0.48	9.4%	7.8%	0.77	0.74	20.6%	11.1%
16	2.07	–	15.8%	–	0.80	–	10.8%	–	1.52	–	28.1%	–
17	–	0.77	–	6.8%	–	0.54	–	8.8%	–	0.89	–	12.7%
20	0.41	0.22	6.3%	5.0%	0.23	0.13	6.5%	5.1%	0.39	0.19	8.8%	1.6%
22	0.40	0.45	5.9%	7.1%	0.26	0.27	7.2%	8.5%	0.35	0.49	0.0%	19.1%
23	–	0.71	–	8.3%	–	0.31	–	9.4%	–	0.58	–	17.4%

7. Conclusion

In the present study, both the vertical and horizontal scale of fluctuation of Singapore Marine Clay have been determined using CPT data carried out on a piece of reclaimed land. To date, the underlying Upper Marine Clay (UMC) and Lower Marine Clay (LMC) are mostly underconsolidated with the load of the reclamation fills placed from 1970s to 1980s. The degree of consolidation varies across the area, leading to differentials in the undrained shear strength in this area. The current undrained shear strength ratios of both UMC and LMC units are similar. The mean values of $S_u/\sigma'_{vo} = 0.2 \pm 0.05$ for both UMC and LMC units in Clusters 2 and 4 (Figure 1(b)) indicate that (i) underconsolidation is the prominent condition, and (ii) the clay units near to drainage boundaries show full degree of consolidation. The mean values of $S_u/\sigma'_{vo} = 0.12 \pm 0.06$ for both UMC and LMC units in Cluster 5 (Figure 1(b)) indicate that the clays units are largely underconsolidated. The clay units on the original shoreline (cluster 1) and in localised reclaimed area (cluster 3) are overconsolidated, with mean values of $S_u/\sigma'_{vo} = 0.31 \pm 0.05$.

Both vertical and horizontal scales of fluctuation have been characterised. Referring to Figures 5–8 and Figure 10–13, autocorrelation coefficients/semi-variogram values in the horizontal direction (i.e. Figures 10–13) are more scattered than those in the vertical direction (i.e. Figures 5–8). This is due to a practical reason. Unlikely in the vertical direction, where CPT readings are taken every 0.1 m in depth, CPTs do not typically follow a fixed spacing in the horizontal direction. In addition, as explained in Section 5, each horizontal lag distance considered in deriving autocorrelation coefficients/semi-variogram values consists of data spanning across five different lag distance values. This is because there are not enough CPTs to ensure enough data pairs for each individual lag distance in the horizontal direction. In fact, this is believed to be a common issue in site investigation. The CPT layout following a small and fixed spacing in the horizontal direction (e.g. Jakasa, Kaggwa, and Brooker 1999), which was usually specifically designed to quantify the horizontal scale of fluctuation, can hardly be implemented in practical engineering. As a result, the combination of data from several lag distance

Table 12. Summary of results of horizontal scale of fluctuation of UMC and LMC considering nugget.

	Exponential				Spherical				Gaussian			
	SoF (*m*)		Nugget/Sill		SoF (*m*)		Nugget/Sill		SoF (*m*)		Nugget/Sill	
Reduced Level| (*m*)	UMC	LMC	UMC	LMC	UMC	LMC	UMC	LMC	UMC	LMC	UMC	LMC
89.3	145.2	–	10.2%	–	111.3	–	14.2%	–	152.1	–	14.4%	–
88.8	163.6	–	11.2%	–	119.1	–	13.6%	–	159.9	–	14.8%	–
88.3	182.0	–	10.1%	–	126.0	–	14.3%	–	168.0	–	15.9%	–
87.8	172.2	–	7.3%	–	119.0	–	14.1%	–	158.9	–	18.2%	–
87.3	178.6	–	10.1%	–	128.5	–	15.6%	–	155.3	–	15.9%	–
86.8	213.2	–	9.3%	–	171.5	–	9.2%	–	213.3	–	9.2%	–
86.3	197.0	–	6.9%	–	172.2	–	6.8%	–	215.0	–	6.8%	–
85.8	232.1	–	6.3%	–	194.6	–	6.2%	–	252.4	–	6.2%	–
84.3	194.1	–	4.5%	–	191.1	–	4.4%	–	206.3	–	4.4%	–
77.4	–	176.6	–	0.2%	–	139.5	–	8.5%	–	185.0	–	14.4%
76.9	–	204.2	–	1.0%	–	195.5	–	7.6%	–	230.9	–	10.1%
76.4	–	177.9	–	0.4%	–	119.7	–	0.2%	–	174.9	–	0.2%
75.9	–	149.4	–	0.5%	–	96.8	–	3.3%	–	157.3	–	11.5%
75.4	–	112.9	–	3.2%	–	83.5	–	4.4%	–	133.0	–	10.3%

values is a practical compromise, but it inevitably introduces uncertainties in the calculated autocorrelation coefficients/semi-variogram values and, therefore, the derived scale of fluctuation.

Nevertheless, the different techniques considered in the present study have generally yielded comparable values of scale of fluctuation. The values of vertical scale of fluctuation are approximately 0.57 ± 0.3 m and 0.48 ± 0.17 m for UMC and LMC, respectively, while the values of horizontal scale of fluctuation are approximately 148 ± 26 m and 138 ± 28 m. Compared to existing geotechnical database of soft marine clay, the derived values of horizontal scale of fluctuation appear to be high. Further investigations are warranted. Nevertheless, this observation is valuable for the reliability analysis of offshore geo-structures because it suggests that neglecting horizontal spatial variation might be acceptable for local-scale projects. Consequently, simplified reliability analyses can be carried out using random fields in 1D instead of 3D.

Furthermore, the degree of consolidation has not been observed to have significant influence on vertical scales of fluctuation of both UMC and LMC units. In addition, the magnitudes of horizontal scale of fluctuation of both UMC and LMC have been shown to be fairly independent of depth. The current study has contributed to the database of spatial variability of natural soils in the literature and provided critical information for reliability assessment of geotechnical structures on Singapore Marine Clay and areas of similar geological settings.

Acknowledgements

This research was supported by the Fundamental Research Funds for the Central Universities (2023ZYGXZR028), European Union's Horizon 2020 research and innovation program under the Marie Skłodowska-Curie grant agreement (grant number 101034337), and Alexander von Humboldt Foundation. The financial support is gratefully acknowledged.

Disclosure statement

No potential conflict of interest was reported by the author(s).

Data availability statement

Some or all data, models, or codes that support the findings of this study are available from the corresponding author upon reasonable request.

ORCID

Ze Zhou Wang http://orcid.org/0000-0002-9907-0193
Xiangfeng Guo https://orcid.org/0000-0002-3266-4325
Yue Hu https://orcid.org/0000-0001-8748-7517

References

Baecher, G. B., M. Chan, T. S. Ingra, T. Lee, and L. R. Nucci. 1980. "Geotechnical Reliability of Offshore Gravity Platforms."

Bong, T., and A. W. Stuedlein. 2017. "Spatial Variability of CPT Parameters and Silty Fines in Liquefiable Beach Sands." *Journal of Geotechnical and Geoenvironmental Engineering* 143 (12): 04017093. https://doi.org/10.1061/(ASCE)GT.1943-5606.0001789

Bong, T., and A. W. Stuedlein. 2018. "Effect of Cone Penetration Conditioning on Random Field Model Parameters and Impact of Spatial Variability on Liquefaction-Induced Differential Settlements." *Journal of Geotechnical and Geoenvironmental Engineering* 144 (5): 04018018. https://doi.org/10.1061/(ASCE)GT.1943-5606.0001863

Box, G. E., G. M. Jenkins, G. C. Reinsel, and G. M. Ljung. 2015. *Time Series Analysis: Forecasting and Control*. Hoboken, New Jersey: John Wiley & Sons.

Ching, J., and K. K. Phoon. 2012. "Establishment of Generic Transformations for Geotechnical Design Parameters." *Structural Safety* 35:52–62. https://doi.org/10.1016/j.strusafe.2011.12.003

Cressie, N. 1992. "Statistics for Spatial Data." *Terra Nova* 4 (5): 613–617. https://doi.org/10.1111/j.1365-3121.1992.tb00605.x

Dasaka, S. M., and L. M. Zhang. 2012. "Spatial Variability of in Situ Weathered Soil." *Géotechnique* 62 (5): 375. https://doi.org/10.1680/geot.8.P.151.3786

Davis, J. C., and R. J. Sampson. 1986. *Statistics and Data Analysis in Geology* (Vol. 646). New York: Wiley.

De Gast, T., P. J. Vardon, and M. A. Hicks. 2021. "Assessment of Soil Spatial Variability for Linear Infrastructure Using Cone Penetration Tests." *Géotechnique* 71 (11): 999–1013. https://doi.org/10.1680/jgeot.19.SiP.002

DeGroot, D. J., and G. B. Baecher. 1993. "Estimating Autocovariance of in-Situ Soil Properties." *Journal of Geotechnical Engineering* 119 (1): 147–166. https://doi.org/10.1061/(ASCE)0733-9410(1993)119:1(147)

Diaz Padilla, J., and E. Vanmarcke. 1974. "Settlement of Structures on Shallow Foundations."

D'Ignazio, M., K. K. Phoon, S. A. Tan, and T. T. Länsivaara. 2016. "Correlations for Undrained Shear Strength of Finnish Soft Clays." *Canadian Geotechnical Journal* 53 (10): 1628–1645. https://doi.org/10.1139/cgj-2016-0037

Fan, M. F. 2015. "Marina Bay Realised." *Asian cities Research*. https://fac.arch.hku.hk/asian-cities-research/marina-bay-realised/.

Fenton, G. A. 1999. "Random Field Modeling of CPT Data." *Journal of Geotechnical and Geoenvironmental Engineering* 125 (6): 486–498. https://doi.org/10.1061/(ASCE)1090-0241(1999)125:6(486)

Fenton, G. A., and D. V. Griffiths. 2002. "Probabilistic Foundation Settlement on Spatially Random Soil." *Journal of Geotechnical and Geoenvironmental Engineering* 128 (5): 381–390. https://doi.org/10.1061/(ASCE)1090-0241(2002)128:5(381)

Firouzianbandpey, S., D. V. Griffiths, L. B. Ibsen, and L. V. Andersen. 2014. "Spatial Correlation Length of Normalized Cone Data in Sand: Case Study in the North

of Denmark." *Canadian Geotechnical Journal* 51 (8): 844–857. https://doi.org/10.1139/cgj-2013-0294

Griffiths, D. V., J. Huang, and G. A. Fenton. 2009. "Influence of Spatial Variability on Slope Reliability Using 2-D Random Fields." *Journal of Geotechnical and Geoenvironmental Engineering* 135 (10): 1367–1378. https://doi.org/10.1061/(ASCE)GT.1943-5606.0000099

Guo, W., X. Tan, J. Zhang, X. Lin, X. Dong, and X. Hou. 2023. "System Reliability and Sensitivity Analysis of Lateral Loaded Pile Considering Soil's Spatial Variability." *Georisk: Assessment and Management of Risk for Engineered Systems and Geohazards* 17 (4): 651–665. https://doi.org/10.1080/17499518.2023.2174264

Honjo, Y. 1982. "A Probabilistic Approach to Evaluate Shear Strength of Heterogeneous Stabilized Ground by Deep Mixing Method." *Soils and Foundations* 22 (1): 23–38. https://doi.org/10.3208/sandf1972.22.23

Hu, Y., and Y. Wang. 2024. "Evaluating Statistical Homogeneity of Cone Penetration Test (CPT) Data Profile Using Auto-Correlation Function." *Computers and Geotechnics* 165:105852. https://doi.org/10.1016/j.compgeo.2023.105852

Huber, M.. 2013. "Soil Variability and its Consequences in Geotechnical Engineering." 69 of the Proceedings the Institute of Geotechnical Engineering at the University of Stuttgart (IGS).

Jaksa, M. B. 1995. *The Influence of Spatial Variability on the Geotechnical Design Properties of a Stiff, Overconsolidated Clay*, Doctoral dissertation.

Jaksa, M. B., P. I. Brooker, and W. S. Kaggwa. 1997. "Modelling the Spatial Variability of the Undrained Shear Strength of Clay Soils Using Geostatistics." In *Proceedings of the Fifth International Geostatistics Congress*, edited by E. Y. Baafi and N. A. Schofield, 1284–1295.

Jaksa, M. B., W. S. Kaggwa, and P. I. Brooker. 1999, December. "Experimental Evaluation of the Scale of Fluctuation of a Stiff Clay." In *Proceedings of the 8th International Conference on the Application of Statistics and Probability*, Vol. 1, edited by R. E. Melchers and M. G. Stewart, 415–422. Sydney: AA Balkema, Rotterdam.

Journel, A. G., and C. J. Huijbregts. 1976. Mining Geostatistics.

Krabbenhoft, K., A. V. Lyamin, J. Krabbenhoft and Optum Computational Engineering (Optum G2). 2015. www.optumce.com.

Larsson, S., H. Stille, and L. Olsson. 2005. "On Horizontal Variability in Lime-Cement Columns in Deep Mixing." *Géotechnique* 55 (1): 33–44. https://doi.org/10.1680/geot.2005.55.1.33

Li, J. Z., S. H. Zhang, L. L. Liu, L. C. Wang, and B. Wang. 2024. "Reliability Analysis and Risk Assessment of Pile-Reinforced Slopes Considering Spatial Soil Variability and Site Investigation." *Georisk: Assessment and Management of Risk for Engineered Systems and Geohazards*, 1–20.

Liu, C. N., and C. H. Chen. 2010. "Estimating Spatial Correlation Structures Based on CPT Data." *Georisk* 4 (2): 99–108.

Lumb, P. 1974. "Application of Statistics in Soil Mechanics." *Soil Mechanics New Horizons. IK Lee, ed.*

Navin, M. P. 2005. *Stability of Embankments Founded on Soft Soil Improved with Deep-mixing-method Columns* (Doctoral dissertation, Virginia Tech).

Nishimura, S., T. Shibata, T. Shuku, and K. Imaide. 2017. "Geostatistical Analysis for Identifying Weak Soil Layers in Dikes." In *Geo-Risk 2017*, edited by J. S. Huang, G. A. Fenton, L. M. Zhang, and D. V. Griffiths, 529–538. Denver, Colorado: ASCE.

Oguz, E. A., N. Huvaj, and D. V. Griffiths. 2019. "Vertical Spatial Correlation Length Based on Standard Penetration Tests." *Marine Georesources & Geotechnology* 37 (1): 45–56. https://doi.org/10.1080/1064119X.2018.1443180

Phoon, K. K., Z. J. Cao, J. Ji, Y. F. Leung, S. Najjar, T. Shuku, … J. Ching. 2022. "Geotechnical Uncertainty, Modeling, and Decision Making." *Soils and Foundations* 62 (5): 101189. https://doi.org/10.1016/j.sandf.2022.101189

Phoon, K. K., and F. H. Kulhawy. 1999. "Characterization of Geotechnical Variability." *Canadian Geotechnical Journal* 36 (4): 612–624. https://doi.org/10.1139/t99-038

Phoon, K. K., S. T. Quek, and P. An. 2003. "Identification of Statistically Homogeneous Soil Layers Using Modified Bartlett Statistics." *Journal of Geotechnical and Geoenvironmental Engineering* 129 (7): 649–659. https://doi.org/10.1061/(ASCE)1090-0241(2003)129:7(649)

Phoon, K. K., S. T. Quek, and P. An. 2004. "Geostatistical Analysis of Cone Penetration Test (CPT) Sounding Using the Modified Bartlett Test." *Canadian Geotechnical Journal* 41 (2): 356–365. https://doi.org/10.1139/t03-091

Pieczyńska-Kozłowska, J. M., M. Chwała, and W. Puła. 2022. "Worst-case Effect in Bearing Capacity of Spread Foundations Considering Safety Factors and Anisotropy in Soil Spatial Variability." *Georisk: Assessment and Management of Risk for Engineered Systems and Geohazards* 17 (2): 330–345. https://doi.org/10.1080/17499518.2022.2046786

Pitts, J. O. H. N. 1992. "Landforms and Geomorphic Evolution of the Islands During the Quaternary." In *Physical Adjustment in a Changing Landscape: The Singapore Story*, edited by A. Gupta and J. Pitts, 83–143. Singapore: Singapore University Press.

Qi, X. H., and H. X. Liu. 2019. "Estimation of Autocorrelation Distances for in-Situ Geotechnical Properties Using Limited Data." *Structural Safety* 79:26–38. https://doi.org/10.1016/j.strusafe.2019.02.003

Sen, P. K. 1968. "Estimates of the Regression Coefficient Based on Kendall's Tau." *Journal of the American Statistical Association* 63 (324): 1379–1389. https://doi.org/10.1080/01621459.1968.10480934

Spry, M. J., F. H. Kulhawy, and M. D. Grigoriu. 1988. *A Probability-Based Geotechnical Site Characterization Strategy for Transmission Line Structures*. Report EL-5507, Vol. 1. Electric Power Research Institute, Palo Alto, 394.

Stuedlein, A. W., S. L. Kramer, P. Arduino, and R. D. Holtz. 2012. "Geotechnical Characterization and Random Field Modeling of Desiccated Clay." *Journal of Geotechnical and Geoenvironmental Engineering* 138 (11): 1301–1313. https://doi.org/10.1061/(ASCE)GT.1943-5606.0000723

Sujawat, R. S., and R. Kumar. 2023. "Stochastic Numerical Analyses to Investigate the Effects of the Spatial Nonuniformity of Offshore Ground on the Serviceability of Monopile Foundations." *Georisk: Assessment and Management of Risk for Engineered Systems and Geohazards* 18 (3): 591–608. https://doi.org/10.1080/17499518.2023.2283849

Tan, T. S., K. K. Phoon, F. H. Lee, H. Tanaka, J. Locat, and P. T. Chong. 2003. "A Characterisation Study of Singapore Lower Marine Clay." *Characterisation and Engineering Properties of Natural Soils* 1:428–464.

Uzielli, M., G. Vannucchi, and K. K. Phoon. 2005. "Random Field Characterisation of Stress-Nomalised Cone Penetration Testing Parameters." *Geotechnique* 55 (1): 3–20. https://doi.org/10.1680/geot.2005.55.1.3

Vanmarcke, E. H. 1977. "Probabilistic Modeling of Soil Profiles." *Journal of the Geotechnical Engineering Division* 103 (11): 1227–1246. https://doi.org/10.1061/AJGEB6.0000517

Wang, C., C. A. Osorio-Murillo, H. Zhu, and Y. Rubin. 2017. "Bayesian Approach for Calibrating Transformation Model from Spatially Varied CPT Data to Regular Geotechnical Parameter." *Computers and Geotechnics* 85:262–273. https://doi.org/10.1016/j.compgeo.2017.01.002

Wang, Y., T. Zhao, Y. Hu, and K. K. Phoon. 2019. "Simulation of Random Fields with Trend from Sparse Measurements Without Detrending." *Journal of Engineering Mechanics* 145 (2): 04018130. https://doi.org/10.1061/(ASCE)EM.1943-7889.0001560

Whittle, A. J., and R. V. Davies. 2006, June. "Nicoll Highway Collapse: Evaluation of Geotechnical Factors Affecting Design of Excavation Support System." In *International Conference on Deep Excavations*, Vol. 28, 30–45. Singapore.

Xu, L., G. Zhou, T. Zhao, and L. Zuo. 2023. "Characterization of Inherent Spatial Variability of Loess Deposit Properties in Shaanxi Province, China." *Journal of Soils and Sediments* 23 (7): 2862–2877. https://doi.org/10.1007/s11368-023-03517-8

Zhao, T. Y., Y. Wang, S. F. Lu, and L. Xu. 2023. "Fast stratification of geological cross-section from CPT results with missing data using multitask and modified Bayesian compressive sensing." *Canadian Geotechnical Journal* 60 (12): 1812–1834. http://dx.doi.org/10.1139/cgj-2022-0131.

Appendix. Modified Bartlett Test

A profile of measurement of interest is said to be weakly stationary if: (i) the mean is constant, and (ii) the autocovariance is only a function of the distance between observations (Phoon, Quek, and An 2003). The second condition is verified if the variance remains constant with position. The Bartlett test is one of the classical tests used to test the equality of two or multiple variances, but this technique assumes that the data are independent (Cressie 1992), which is antithetical to the known correlation structure in spatially varying soil parameters. As a result, Phoon, Quek, and An (2003) proposed a new statistical test, modified Bartlett test (MBS), and the accompanying rejection criteria to assess stationarity for correlated data at 5% significance level.

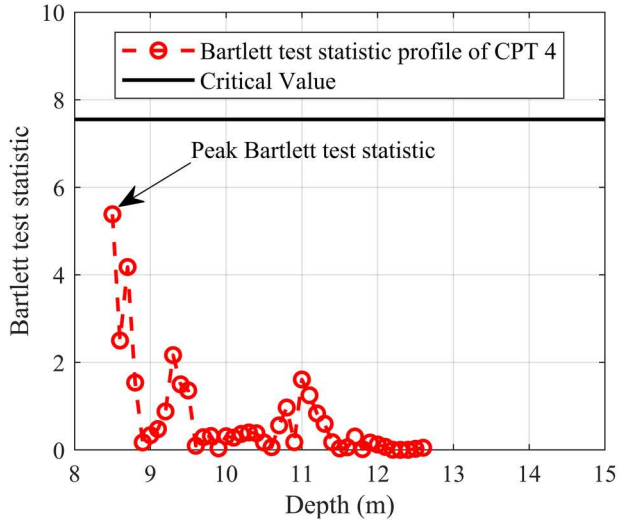

Figure A1. Example of Bartlett test statistic profile.

This technique starts from moving a sampling window over a given CPT profile. For each moving step, the sampling window is divided into two equal segments and the sample variances of the data points lying within each segment can be calculated. It is recommended by Phoon, Quek, and An (2003) that each segment should at least cover 10 data points to ensure that the sample variances can be estimated reasonably accurately. The classic Bartlett test is then carried out to test the difference between these two values of sample variances (from the two segments) and the Bartlett test statistic is recorded. After the sampling window screens the entire CPT profile, a continuous Bartlett test statistic profile can be obtained. The peak Bartlett test statistic value is then compared with a critical value for rejection or acceptance of the stationary hypothesis at 5% significance level. The estimation of the critical value was developed by Phoon, Quek, and An (2003) numerically through a series of simulations and summarised into a convenient form for practical use.

Figure A1 shows an example of the MBS analysis using the UMC profile of CPT 4 (e.g. Figure 4a). A continuous Bartlett test statistic profile was first obtained using a sampling window of size 20, and the peak value was found to be approximately 5.4, which is lower than the critical value of 7.6. Therefore, this set of data is deemed to pass the modified Bartlett test at 5% significance level. Similar procedures were followed to obtain the results summarised in Tables 4 and 5.